ELSEVIER

Int. J. Electron. Commun. (AEÜ) **58** (2004): 391–401
http://www.elsevier.de/aeue

International Journal AEÜ of **Electronics** and **Communications**

Automatic Step-size Control in Wave Digital Simulation Using Passive Numerical Integration Methods

Dietrich Fränken and Karlheinz Ochs

Abstract: Wave digital filter principles can be applied to the numerical solution of many kinds of differential equations. It has been shown that, by merging the wave digital concept with RUNGE-KUTTA methods, algorithms of high accuracy can be found which are passive and hence possess a lot of desirable numerical stability properties. In this paper, we will discuss the applicability of step-size control within this framework.

Keywords: Wave digital simulation, Passive integration methods, RUNGE-KUTTA methods, Step-size control

1. Introduction

A large variety of methods for the numerical integration of differential equations exists. It has been shown that the application of principles formerly introduced for so-called wave digital filters (for an overview, see [1]) may be viewed as a numerical integration of KIRCHHOFF network equations by means of specific linear multistep methods [2]. The resulting algorithms possess some advantageous numerical features which are implied by a property called passivity where the latter can be ensured even under finite word-length conditions. The principles may be applied to both linear or non-linear ordinary or partial differential equations as long as these can be represented by KIRCHHOFF networks, cf. [2–6]. In recent publications, it has been shown that the application of appropriate RUNGE-KUTTA methods within this framework may yield, at least for ordinary differential equations, an increased numerical accuracy without sacrificing passivity and the stability properties induced herewith [7–9].

In this context, only numerical integration with fixed step-sizes has been considered until now. But, it is known that such a restriction may cause unsatisfactory simulation results if the system of differential equations under investigation constitutes a stiff problem. In lack of a precise mathematical definition, a problem is commonly called stiff if its solution consists of both *transient* as well as *smooth* phases, i.e. if the occuring signals change rapidly during some time intervals and vary only slowly during others. Now, a step-size being appropriately adjusted for the transient phases turns out to be unnecessarily small for the smooth phases which causes long simulation times and a high accumulation of (unavoidable) rounding errors. On the other hand, a (larger) step-size adjusted to the smooth phases in general does not allow for a detailed replication of transient components in the signals and, depending on the chosen integration method, may even cause completely useless simulation results. If both transient and smooth phases are to be simulated with good time resolution, the usage of an adaptively varying step-size is indispensable.

In this paper, it is shown that wave digital simulation with variable step-sizes is indeed possible, again without sacrificing passivity as the key property. We start our presentation by briefly recalling the basic wave digital simulation principles. The application of linear multistep methods and of RUNGE-KUTTA methods in this framework is shortly explained and the passivity concept for these methods is recalled. It is demonstrated that, even for wave digital structures which are known to be stable for each possible fixed step-size, an incautious variation of those parameters depending on the step-size may cause an instable behaviour. It is also discussed how this problem can be overcome by a suitable modification of the way certain reactive elements are represented in the KIRCHHOFF network. In combination with suitable RUNGE-KUTTA methods, the general possibility of a passive numerical integration with variable step-sizes is thus established.

We continue our presentation with a short explanation of a standard approach which can be used for step-size selection. A new passive RUNGE-KUTTA method is presented which is designed to meet the requirements imposed by the chosen approach. Simulation results obtained by means of wave digital simulation using this method with both variable and fixed step-sizes conclude this paper.

2. Wave digital simulation principles

The standard procedure to simulate a circuit by means of wave digital structures is as follows: First, the circuit is decomposed into oneports and multiports where to each port a *port resistance* is assigned being a positive constant. Now, so-called (voltage) *wave quantities* are introduced, i. e., for a port with voltage v_ν, current i_ν, and port resis-

Received December 17, 2002. Revised January 8, 2004.

D. Fränken, EADS Deutschland GmbH, Wörthstr. 85, 89077 Ulm, Germany. E-mail: fraenken@ieee.org.
K. Ochs, Department of Electrical Engineering and Information Technology/Communications Engineering, Ruhr-University, 44780 Bochum, Germany. E-mail: ochs@ieee.org.

Corresponding to: D. Fränken

1434-8411/04/58/06-391 $ 30.00/0

tance R_ν, one defines

$$a_\nu := v_\nu + R_\nu i_\nu \quad \text{and} \quad b_\nu := v_\nu - R_\nu i_\nu. \tag{1}$$

The equations imposed by both the static network elements as well as KIRCHHOFF laws can immediately (without any approximation) be rewritten in dependence on these wave quantities. With suitably chosen port resistances, a resistive voltage source becomes a wave source and a resistance results in a wave sink. The KIRCHHOFF equations describing parallel or series connections are realized by so-called parallel and series adaptors [1], more general connection types can also be dealt with [10, 11]. Reactive (and hence dynamic) elements have to be treated by applying an appropriate numerical integration method in order to find approximate solutions. Although we will restrict the presentation to linear and non-coupled capacitances and inductances in the sequel, it is noteworthy that the principles can also be applied to networks wich include nonlinear and/or coupled reactive elements as these (lossless) elements can be represented by linear reactive one-port elements in combination with linear or nonlinear (non-energic) transformer multiports (see e.g. [6, 12]).

2.1 Linear multistep methods

Consider a KIRCHHOFF network which, in addition to a voltage source and a single capacitance, only contains non-dynamic and source-free elements. Then, the voltage v and the current i at the capacitance are described by the differential equation

$$\dot{v}(t) = C^{-1} i(t) \quad \text{with} \quad v(t_0) = v_0\,, \tag{2a}$$

while the other elements are assumed to impose a (possibly nonlinear) algebraic equation of the form

$$C^{-1} i(t) = f(v(t), x(t)) \tag{2b}$$

where $x(t)$ is the source voltage.

Now, a linear multistep method numerically solves the differential equation (2a) by replacing it with the difference equation

$$v(t_k) = -\sum_{\sigma=1}^{s} \alpha_\sigma v(t_{k-\sigma}) + TC^{-1} \sum_{\sigma=0}^{s} \beta_\sigma i(t_{k-\sigma}) \tag{3a}$$

with

$$C^{-1} i(t_k) = f(v(t_k), x(t_k)) \tag{3b}$$

where α_σ, β_σ are suitably chosen parameters, T is the step-size or sampling period, and the time instances t_k are defined by $t_k := t_0 + kT$ with $k \in \mathbb{Z}$. Here, it is common practice to consider the steady state at some complex frequency p where v and i are assumed to be of the form $v(t_k) := V\mathrm{e}^{pt_k}$ and $i(t_k) := I\mathrm{e}^{pt_k}$, respectively [2, 13, 14]. In this case, the linear difference equation yields $V = RZ(\psi)I$ with

$$Z(\psi) := 2 \sum_{\sigma=0}^{s} \beta_\sigma \left[\frac{1-\psi}{1+\psi}\right]^\sigma \Bigg/ \sum_{\sigma=0}^{s} \alpha_\sigma \left[\frac{1-\psi}{1+\psi}\right]^\sigma \tag{4}$$

(with $\alpha_0 := 1$) where

$$\psi := \tanh(pT/2) = \frac{\mathrm{e}^{pT} - 1}{\mathrm{e}^{pT} + 1} \tag{5}$$

denotes the so-called *equivalent complex frequency* and

$$R := \frac{T}{2C} \tag{6}$$

is a normalization resistance. The term $Z(\psi)$ is called the (normalized) *characteristic impedance* of the linear multistep method [7] and is assumed to be of irreducible form.

Traditionally, the trapezoidal rule with characteristic impedance $Z(\psi) = 1/\psi$ is used within the wave digital concept. In combination with Eq. (1) for a port resistance chosen as in Eq. (6), the difference equation (3a) then simplifies to

$$b(t_k) = a(t_{k-1}), \tag{7}$$

and the wave digital realization of a capacitance is a mere time delay. Likewise, an inductance L with port resistance $2L/T$ yields a time delay in combination with an additional sign inverter. For networks with multiple reactive elements, each of these reactive elements is replaced accordingly. In case other linear multistep methods than the trapezoidal rule are to be used, port resistances for capacitance and inductance are chosen as $R_C = Z(1)T/[2C]$ and $R_L = 2L/[Z(1)T]$, respectively, and each time delay has finally to be substituted by a wave digital structure with *characteristic reflectance*

$$S(\psi) = \frac{Z(\psi) - Z(1)}{Z(\psi) + Z(1)}. \tag{8}$$

Clearly, $Z(1) \neq 0 \iff \beta_0 \neq 0$ holds here and thus *implicit methods* must be used.

In Fig. 1, the result of the described procedure is shown for a series connection of a resistive voltage source, a capacitance, and an inductance where R_x, C, and L are positive constants. As indicated by a $\perp$-formed symbol, the aforementioned choice of port resistances for the reactive elements yields, with $S(1) = 0$, *reflection-free* connection ports, i.e., ports without any delay-free directed path between input and output. Hence, the given signal flow diagram does not contain any delay-free directed loop and thus is *computable*.

2.2 RUNGE-KUTTA methods

The application of a RUNGE-KUTTA method [15] to Eq. (2a) yields

$$\boldsymbol{v}(t_k) = \boldsymbol{e}v(t_k) + 2R\boldsymbol{D}\boldsymbol{i}(t_k) \tag{9a}$$

$$v(t_{k+1}) = v(t_k) + 2R\boldsymbol{g}^{\mathrm{T}}\boldsymbol{i}(t_k) \tag{9b}$$

with $\boldsymbol{e} = [1, \ldots, 1]^{\mathrm{T}}$ and R as in Eq. (6) where some parameters of the method are combined in vector $\boldsymbol{g}$ and matrix $\boldsymbol{D}$ of appropriate dimensions. For a method with s stages, the vectors $\boldsymbol{v}$ and $\boldsymbol{i}$ consist of s stage voltages v_σ and s stage currents i_σ, respectively, which are related by

$$C^{-1}i_\sigma(t_k) = f(v_\sigma(t_k), x(t_k + k_\sigma T)) \tag{9c}$$

with nodes k_σ and the same function f as given in Eq. (2b).

Here, a steady-state analysis of Eqs. (9) yields a relation $\boldsymbol{V} = R\boldsymbol{Z}(\psi)\boldsymbol{I}$ with

$$\boldsymbol{Z}(\psi) = \frac{\boldsymbol{e}\boldsymbol{g}^{\mathrm{T}}}{\psi} + 2\boldsymbol{D} - \boldsymbol{e}\boldsymbol{g}^{\mathrm{T}} \tag{10}$$

where $\boldsymbol{Z}(\psi)$ is the so-called (normalized) *characteristic impedance matrix* [7]. The corresponding *characteristic scattering matrix* is given by

$$\boldsymbol{S}(\psi) = [\boldsymbol{Z}(\psi) - \boldsymbol{R}][\boldsymbol{Z}(\psi) + \boldsymbol{R}]^{-1} \tag{11}$$

where $\boldsymbol{R}$ is the diagonal matrix of port resistances which, again for reasons of computability, must be chosen equal to the diagonal entries of $\boldsymbol{Z}(1)$.

Fig. 2 shows how a wave digital simulation with a two-stage RUNGE-KUTTA method can be performed for the circuit in Fig. 1. To this end, the inductance L has equivalently been replaced by a gyrator with gyration resistance R_{G} which is terminated with a capacitance L/R_{G}^2. In the wave digital structure, each capacitance is represented by a two-port with a scattering matrix as given in Eq. (11). The wave source and the series adaptor, which account for the equations related to the non-dynamic part of the network, now occur twice. Herein, the two copies are structurally equal – we will comment on this in more detail later on – and differ with respect to a time shift of their input signals only.

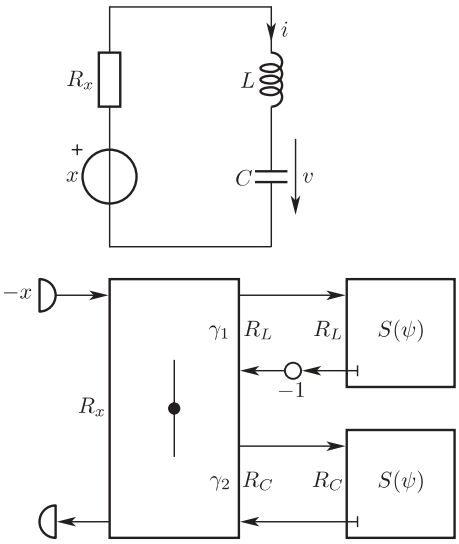

Fig. 1. KIRCHHOFF network and its discrete-time equivalent after application of a linear multistep method. Port resistances are R_x, $R_C = Z(1)T/[2C]$, and $R_L = 2L/[Z(1)T]$.

From Fig. 2, it becomes apparent that additional requirements have to be met by the RUNGE-KUTTA method in order to ensure computability. In fact, the occurrence of delay-free directed loops now requires $\boldsymbol{S}(1)$ to be of strict lower (or upper) triangular form. With the choice of port resistances given above, this requirement is met by considering so-called *diagonally implicit* methods only for which, by definition, $\boldsymbol{D} = \boldsymbol{Z}(1)/2$ is of lower triangular form. In this case, no delay-free directed path leads from the adaptor on the right to the one on the left hand side. Consequently, the two sub-structures can, from left to right, be computed sequentially.

2.3 Some implementation aspects

With the results of the previous sections, a flexible and user-friendly implementation of wave digital simulation principles can be obtained. For a given KIRCHHOFF net-

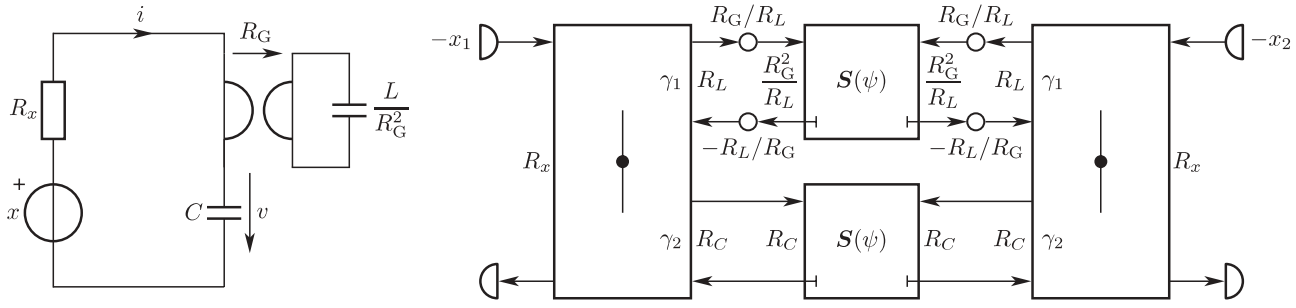

Fig. 2. KIRCHHOFF network equivalent to the one in Fig. 1 and its discrete-time representation after application of a two-stage RUNGE-KUTTA method. There holds $x_1(t_k) = x(t_k + k_1 T)$ and $x_2(t_k) = x(t_k + k_2 T)$ as well as $R_C = Z_{11}(1)T/[2C]$ and $R_L = 2L/[Z_{11}(1)T]$.

work, a wave digital model function has to be provided which covers the non-dynamic part of the network (including all connections) and thus relates the wave quantities emitted by the reactive elements with those reflected back into them just the way it is standard when the trapezoidal rule is used. The corresponding signal flow diagram is fixed in structure, but adaptor and other coefficients depend on the actual port resistances and source values must be computed according to the relevant time-shift. Within each time step, the function is called once (for a linear multistep method or a one-stage RUNGE-KUTTA method) or several times (for multistage RUNGE-KUTTA methods) by the integrating routine – this routine is the realization of the *characteristic oneport* or *multiport*, respectively – and thus solves Eqs. (3b) or (9c) in the wave domain. The computation of coefficients depending on the port resistances has to be performed only when starting simulation, either once in total (for linear multistep methods or for RUNGE-KUTTA methods with equal diagonal entries of $\boldsymbol{Z}(1)$) or once per stage (for RUNGE-KUTTA methods with differing diagonal entries of $\boldsymbol{Z}(1)$). Thus, in comparison with a general diagonally implicit RUNGE-KUTTA method, the usage of a method having equal diagonal elements in $\boldsymbol{Z}(1)$ and hence in $\boldsymbol{D}$ leads to a reduced computational effort. Such a method is called *singly diagonally implicit* and has already been used in Fig. 2 for the sake of a compact presentation.

The wave digital model function discussed here may be supplied by the user, but can also, for many KIRCHHOFF networks, be generated automatically from a given netlist [11].

3. Passive methods

For a wave digital simulation, so-called *passive methods* are of particular importance where a numerical integration method is called passive if the corresponding characteristic impedance (matrix) represents a passive (discrete-time) network [7, 9]. Hence, a linear multistep method is passive if the corresponding characteristic impedance is a positive function, i. e., if the implication

$$\operatorname{Re}\psi > 0 \quad \Rightarrow \quad \operatorname{Re} Z(\psi) \geq 0 \tag{12}$$

holds. Analogously, a RUNGE-KUTTA method is passive if its characteristic impedance matrix is positive, i. e., if

$$\operatorname{Re}\psi > 0 \quad \Rightarrow \quad \boldsymbol{Z}(\psi) + \boldsymbol{Z}^{*}(\psi) \geq \boldsymbol{0} \tag{13}$$

is fulfilled. The application of a passive method to a KIRCHHOFF network consisting of passive elements in addition to resistive sources only yields a wave digital structure which again contains, in addition to wave sources, only passive elements. Among other properties, this implies

$$\boldsymbol{w}_{k+1}^{\mathrm{T}}\boldsymbol{G}\boldsymbol{w}_{k+1} - \boldsymbol{w}_{k}^{\mathrm{T}}\boldsymbol{G}\boldsymbol{w}_{k} \leq \boldsymbol{x}_{k}^{\mathrm{T}}\boldsymbol{G}_{\boldsymbol{x}}\boldsymbol{x}_{k} \tag{14}$$

where the vector $\boldsymbol{w}_k$ comprises all state values $w_\nu(t_k)$ and $\boldsymbol{G}$ is the (positive definite) diagonal matrix of the corresponding port conductances $G_\nu = 1/R_\nu$ while $\boldsymbol{x}_k$ denotes the vector of all source values $x_\mu(t_k)$ with the associated port conductance matrix $\boldsymbol{G}_{\boldsymbol{x}}$. By simple means, the validity of relation (14) can even be conserved under finite-wordlength conditions [1]. Because the *stored energy* $\boldsymbol{w}_k^{\mathrm{T}}\boldsymbol{G}\boldsymbol{w}_k$ is monotonically decreasing for zero input, one finds that the wave digital structure, in particular, represents a system with an equilibrium $\boldsymbol{0}$ being stable (in the sense of LIAPUNOV) due to passivity.

Now, passive methods also possess certain desirable numerical stability properties. In fact, a linear multistep method is passive if and only if it possesses a property known as A-stability. But, it is known that A-stability of such a method in turn limits the numerical accuracy obtainable for a given step-size. More precisely, the *consistency order* – a measure commonly used to estimate the method's asymptotic behavior for small step-sizes – of an A-stable linear multistep method cannot exceed two (DAHLQUIST's second barrier [16]). However, it has been shown that the maximum attainable consistency order for wave digital simulation can be increased to four by using diagonally implicit passive RUNGE-KUTTA methods [7]. Here, passive methods are always algebraically stable and hence possess one of the most important numerical stability properties one may require for a RUNGE-KUTTA method [17]. Consequently, we will set our focus on these methods from now on.

Passivity imposes certain restrictions on the parameters in $\boldsymbol{D}$ and $\boldsymbol{g}^{\mathrm{T}}$. It has been shown [18] that a RUNGE-KUTTA method is passive if and only if one can write

$$\boldsymbol{g}^{\mathrm{T}} = r\boldsymbol{e}^{\mathrm{T}} \tag{15a}$$

and

$$\boldsymbol{D} = \frac{1}{2}\left[r\boldsymbol{e}\boldsymbol{e}^{\mathrm{T}} + \boldsymbol{\mathcal{R}} + \boldsymbol{\mathcal{S}}\right] \tag{15b}$$

with

$$\boldsymbol{\mathcal{R}} = \boldsymbol{N}\operatorname{diag}(r_\sigma)\boldsymbol{N}^{\mathrm{T}} \quad \text{and} \quad \boldsymbol{\mathcal{S}} = \boldsymbol{L} - \boldsymbol{L}^{\mathrm{T}} \tag{15c}$$

where the (real) parameters are restricted according to

$$\begin{gathered} r > 0, \quad r_\sigma \geq 0, \quad n_{\varrho\sigma} = 0 \ \text{ for } \ \varrho < \sigma, \\ n_{\sigma\sigma} = 1, \quad \text{and} \quad l_{\varrho\sigma} = 0 \ \text{ for } \ \varrho \leq \sigma. \end{gathered} \tag{15d}$$

In most interesting cases, there holds $r_\sigma = 0$ for $\sigma \geq 2$ and $n_{\varrho,1} \neq 0$ for $\varrho = 1, \ldots, s$. Then, the characteristic impedance matrix of a diagonally implicit method can be written according to

$$\begin{aligned} \boldsymbol{Z}(\psi) = {} & [\boldsymbol{1} + \boldsymbol{S}_0(\psi)][\boldsymbol{1} - \boldsymbol{S}_0(\psi)]^{-1}\boldsymbol{R}_0 \\ & + [\boldsymbol{1} + \boldsymbol{S}_1][\boldsymbol{1} - \boldsymbol{S}_1]^{-1}\boldsymbol{R}_1 \end{aligned} \tag{16a}$$

with

$$\boldsymbol{S}_0(\psi) = \begin{bmatrix} \boldsymbol{0}^{\mathrm{T}} & \frac{1-\psi}{1+\psi} \\ \boldsymbol{1} & \boldsymbol{0} \end{bmatrix} \tag{16b}$$

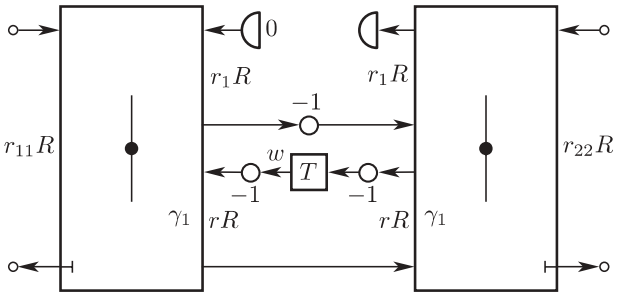

Fig. 3. Wave digital realization of the characteristic two-port for a passive 2-stage RUNGE-KUTTA method.

and

$$\boldsymbol{S}_1 = \begin{bmatrix} \mathbf{0}^{\mathrm{T}} & 0 \\ \mathrm{diag}\left(\frac{n_{\varrho,1}}{n_{\varrho-1,1}}\right) & \mathbf{0} \end{bmatrix}, \quad \varrho = 2, \ldots, s \qquad (16c)$$

where all diagonal entries of the diagonal matrix $\boldsymbol{R}_0$ equal r and the corresponding entries of $\boldsymbol{R}_1$ are $r_1 n_{\varrho,1}^2$, respectively. From this, a wave digital structure for the realization of the characteristic multiport is easily deduced, it consists of two s-ports with scattering matrices $\boldsymbol{S}_0(\psi)$ and $\boldsymbol{S}_1$, respectively, where the two ports belonging to each particular stage are connected via a series adaptor.

Fig. 3 displays the wave digital realization of the characteristic multiport for a specific passive diagonally implicit RUNGE-KUTTA method with two stages. Here, a method has been chosen where, in particular, $n_{21} = -1$ and thus $Z_{11}(1) = Z_{22}(1) = r + r_1$ holds which again, like in Fig. 2, constitutes a singly diagonally implicit method. However, it should be noted that, in general, neither the restriction $r_{11} = \ldots = r_{ss}$ nor the assumptions $r_\sigma = 0$ for $\sigma \geq 2$ and $n_{\varrho\sigma} \neq 0$ for $\varrho = \sigma, \ldots, s$ must be fulfilled in order to find an appropriate wave digital structure. Here, a universal synthesis prodecure exists [12], and a more detailed analysis shows that, within such a structure, the sought approximate solution for a voltage at a capacitance always equals the wave quantity stored in the associated time delay. At the beginning of a simulation, the time delay can thus be fed directly with the initial voltage value and, due to this, wave digital simulation with passive RUNGE-KUTTA methods does not require any additional starting phase for finding appropriate initial values as opposed to most linear multistep methods.

4. Varying step-sizes

Up to this point, we have assumed the step-size T to be constant throughout simulation time. In the following, we wish to consider varying step-sizes as well. This means that the port conductance matrix $\boldsymbol{G}$ associated with the states of the system does now in general depend on the actual step-size. Although, in analogy to relation (14), one now has

$$\boldsymbol{w}_{k+1}^{\mathrm{T}} \boldsymbol{G}_k \boldsymbol{w}_{k+1} - \boldsymbol{w}_k^{\mathrm{T}} \boldsymbol{G}_k \boldsymbol{w}_k \leq \boldsymbol{x}_k^{\mathrm{T}} \boldsymbol{G}_{\boldsymbol{x}} \boldsymbol{x}_k \qquad (17)$$

with some positive definite matrix $\boldsymbol{G}_k$ varying with time, this alone does not ensure stability of the wave digital structure under all circumstances. But, we will see that the procedure for applying passive RUNGE-KUTTA methods proposed in this paper does indeed conserve all the positive features induced by passivity.

In order to illustrate both the possible problems which may arise due to varying port conductances as well as the way we are able to avoid them, consider the two wave digital structures shown in Fig. 4. Both originate from the KIRCHHOFF network displayed in Fig. 1. In Fig. 4(a), the trapezoidal rule (with fixed step-size) has been applied to the unmodified network while, in Fig. 4(b), the one-stage GAUSS method ($k_1 = d_{11} = 1/2$, $g_1 = 1$) has been applied to the network which has been modified as indicated in Fig. 2. The strong similarity between the two realizations is due to the fact that both methods share the same characteristic impedance $Z(\psi) = 1/\psi$. In fact, both structures would (up to a time shift of the input signal) be identical if the gyration resistance were chosen to be $R_{\mathrm{G}} = R_L = 2L/T$ (clearly, this would require the step-size to be fixed).

Now, assume that the port resistances R_L and R_C of the structure in Fig. 4(a) are (arbitrarily) altered during simulation time (note that this does *not* correspond to the application of the trapezoidal rule with variable step-size because, due to the altering port resistances, the sought numerical solutions i and v cannot be obtained from Eq. (1) as usual). For example, choose the (always

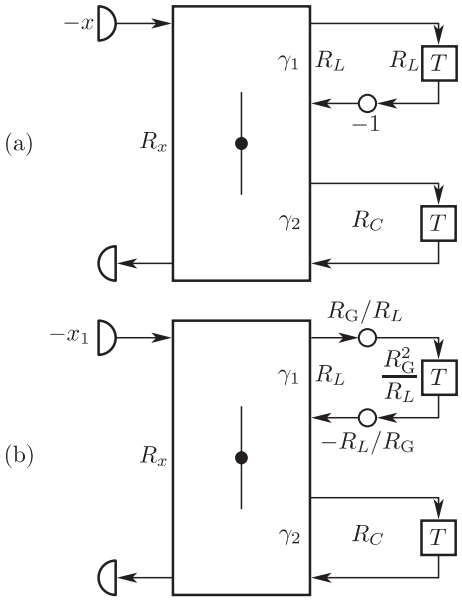

Fig. 4. Discrete-time equivalent to the circuit in Fig. 1 after application of the trapezoidal rule and the one in Fig. 2 after application of the GAUSS method.

positive) port resistances in dependence on the wave quantities a_L and a_C according to

$$R_L(t_k) = \frac{2L}{T_k} \quad \text{and} \quad R_C(t_k) = \frac{T_k}{2C} \tag{18a}$$

with

$$T_k := T(t_k) = T_{\min} + \frac{[T_{\max} - T_{\min}]a_L^2(t_k)}{a_L^2(t_k) + a_C^2(t_k)} \tag{18b}$$

such that T_k stays in the interval $T_{\min} \leq T_k \leq T_{\max}$. Fig. 5 depicts the resulting value a_L of the wave quantity associated with the inductance as a function of time. Herein, the parameters were chosen to be $R_x = 50\,\Omega$, $C = 4.7\,\text{nF}$, $L = 100\,\text{mH}$, $T_{\min} = 340\,\text{ns}$, $T_{\max} = 6.8\,\mu\text{s}$, $a_L(0) = 1\,\text{V}$, and $a_C(0) = 0\,\text{V}$ with zero input. For this set of parameters, the network equations are known to yield damped oscillations with exponentially decreasing envelopes for the states.

As the result confirms, the structure does indeed show an unstable behavior although, with $\boldsymbol{w} := [a_L, a_C]^{\mathrm{T}}$ and $\boldsymbol{G}_k := \operatorname{diag}(1/R_L, 1/R_C)$, relation (17) holds with

$$\boldsymbol{w}_k^{\mathrm{T}} \boldsymbol{G}_k \boldsymbol{w}_k = \frac{T_k}{2L} a_L^2 + \frac{2C}{T_k} a_C^2. \tag{19}$$

This behavior is due to the fact that, with transition from T_k to T_{k+1} and hence from $\boldsymbol{G}_k$ to $\boldsymbol{G}_{k+1}$, the stored energy can get larger both for increasing as well as for decreasing T_k depending on the actual values of the state-variables. For large magnitudes of a_L (relative to $|a_C|$ under consideration of L and C), a change from smaller to larger T_k increases the stored energy and the very same happens when decreasing T_k for relatively small $|a_L|$ and thus large magnitudes of a_C. Obviously, the increase of stored energy due the alteration of T_k according to Eq. (18) here dominates the dissipation of energy due to the resistance which, in total, causes the observed behavior.

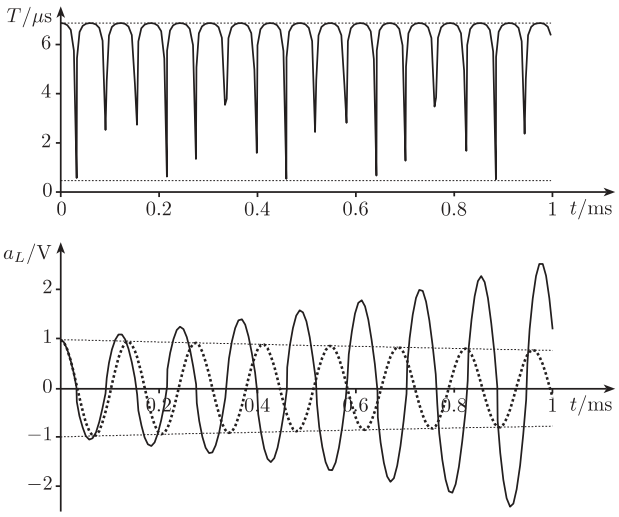

Fig. 5. Wave quantity a_L in the structure in Fig. 4(a) (solid line) and the one in Fig. 4(b) (dashed line) for varying values T.

Now, the wave digital structure in Fig. 4(b) shows a completely different behavior. For reasons of comparability, we have left the parameters of the previous simulation unaltered (with $R_{\mathrm{G}} = 1\,\Omega$) and have also again used the values T_k found therein for altering the port resistances. Fig. 5 confirms that the numerical solution now behaves as desired and, because the wave quantities stored in the time delays equal $R_{\mathrm{G}} i$ and v, respectively, the procedure does indeed correspond to an application of the GAUSS method with variable step-sizes. In this case, the stored energy takes on the form

$$\boldsymbol{w}_k^{\mathrm{T}} \boldsymbol{G}_k \boldsymbol{w}_k = \frac{2L}{R_{\mathrm{G}}^2 T_k} a_L^2 + \frac{2C}{T_k} a_C^2. \tag{20}$$

As we can see, a decreasing step-size T_k now increases the stored energy regardless of the actual state values while an increasing step-size T_k always has the opposite effect. Hence, an alteration of the step-size only causes a fluctuation in the stored energy according to

$$\boldsymbol{w}_k^{\mathrm{T}} \boldsymbol{G}_k \boldsymbol{w}_k = \frac{T_0}{T_k} \boldsymbol{w}_k^{\mathrm{T}} \boldsymbol{G}_0 \boldsymbol{w}_k \tag{21}$$

with the constant matrix $\boldsymbol{G}_0$ and we may thus, in general, write

$$\boldsymbol{w}_{k+1}^{\mathrm{T}} \boldsymbol{G}_0 \boldsymbol{w}_{k+1} - \boldsymbol{w}_k^{\mathrm{T}} \boldsymbol{G}_0 \boldsymbol{w}_k \leq \frac{T_{\max}}{T_0} \boldsymbol{x}_k^{\mathrm{T}} \boldsymbol{G}_{\boldsymbol{x}} \boldsymbol{x}_k \tag{22}$$

for $T_k \leq T_{\max}$. This way, we again are able to prove stability of the equilibrium $\mathbf{0}$ as the step-size is always limited from above (either by a reasonable step-size control or by the absolute desired simulation time).

In addition to the formal investigation thus performed, the example in Fig. 4(b) does also allow for another interpretation. Consider the structure when T is replaced with T_0 in both port resistances R_C and R_{G}^2/R_L while $R_{\mathrm{G}} T_0/T$ is substituted for the gyration resistance R_{G} (thus yielding a port resistance $R_L T_0/T$ instead of R_L at port 1 of the adaptor) as well as $R_x T_0/T$ for the source resistance R_x. Now, observe that adaptor coefficients only depend on *ratios of port resistances* like e.g.

$$\gamma_v = \frac{2R_v}{R_1 + R_2 + R_3} \tag{23}$$

in case of the three-port series adaptor and, consequently, all coefficients in the structure remain unchanged. In other words, the GAUSS method leads to the very same discrete-time structure (up to a different time scaling which cleary does not have any influence on passivity) when applied with fixed step-size T_0 to a circuit containing, in addition to two constant capacitances, a time-variant gyrator and a source with varying (positive) source resistance. But, the dependence on time does not have any influence on the basic energic properties of both the resistance and the gyrator. The former is always passive (as long as it remains positive) while the latter is in any case non-energic.

Hence, passivity of the wave digital structure can also be explained by the usual line of arguments referring to the passivity of the continuous-time KIRCHHOFF network which is to be simulated.

Now, observe that, regardless of the way a valid wave digital structure has been obtained in the first place (e.g. by applying a general passive RUNGE-KUTTA method to a specific KIRCHHOFF network), one can always deduce a (usually different) KIRCHHOFF network from there that, in combination with the GAUSS method, results in the very same wave digital structure. With this interpretation at hand, it becomes apparent that the results stated within this section remain valid for general passive RUNGE-KUTTA methods. Herein, it has been essential for passivity to treat both types of reactive elements (i.e. inductances and capacitances) in a unified manner (by using a suitable replacement for inductances). It should be emphasized at this point that, in contrast to a fixed step-size scenario, adaptor and other coefficients depending on the now varying port resistances have to be recomputed within each time step.

5. Step-size selection

With the general possibility of a passive numerical integration using diagonally implicit RUNGE-KUTTA methods with variable step-sizes, a suitable step-size selection has to be performed. A large variety of algorithms exists for both estimating the current simulation error as well as for a subsequent selection of the step-size in order to limit this error. In the following, we will make use of so-called *embedded methods* for error estimation while applying an elementary algorithm for the actual step-size control.

We start with a short recapitulation of the standard step-size control algorithm presented in [19]. The algorithm tries to adjust the step-size in order to achieve a prescribed tolerance of the so-called *local discretization error*, i.e. the error induced by the application of a RUNGE-KUTTA method within one time step. To this end, two approximate solutions $\boldsymbol{w}(t_k+T)$ and $\hat{\boldsymbol{w}}(t_k+T)$ are computed with a given step-size T where, for now, it is assumed that $\hat{\boldsymbol{w}}(t_k+T)$ is a much better estimate for the exact solution than $\boldsymbol{w}(t_k+T)$. The goal is to have componentwise

$$|w_\nu(t_k+T)-\hat{w}_\nu(t_k+T)| \le \delta_\nu(t_k,T) \tag{24a}$$

with

$$\delta_\nu(t_k,T) := \delta_{\text{abs}} + \max(|w_\nu(t_k+T)|, |w_\nu(t_k)|)\cdot\delta_{\text{rel}} \tag{24b}$$

where the positive values δ_{abs} and δ_{rel} allow for a prescription of absolute and relative error, respectively (different constants $\delta_{\text{abs},\nu}$ and $\delta_{\text{rel},\nu}$ may be used for each component in (24b)). As a measure of error,

$$\varepsilon(t_k,T) := \|\boldsymbol{\epsilon}(t_k,T)\| \tag{25a}$$

with the components

$$\epsilon_\nu(t_k,T) := \frac{|w_\nu(t_k+T)-\hat{w}_\nu(t_k+T)|}{\delta_\nu(t_k,T)} \tag{25b}$$

of $\boldsymbol{\epsilon}(t_k,T)$ is used where $\|\cdot\|$ denotes an appropriate vector norm with $\|\boldsymbol{e}\|=1$ (with this normalization, one has $\varepsilon(t_k,T)=1$ if equality holds in (24a) for all ν). Provided that $\boldsymbol{w}(t_k)$ coincides with the exact solution, $\varepsilon(t_k,T)$ asymptotically behaves similar to the local discretization error. This means that, for small step-sizes, one may write $\varepsilon(t_k,T)\approx\bar{\varepsilon}\,T^{q+1}$ with some constant $\bar{\varepsilon}$ when a method with consistency order q is used for determining the less prescise estimate $\boldsymbol{w}(t_k+T)$.

With the chosen measure of error, one tries to estimate an *optimal step-size* T_{opt} from the requirement $\varepsilon(t_k,T_{\text{opt}})\lessapprox 1$ and thus from

$$1\approx\bar{\varepsilon}T_{\text{opt}}^{q+1} \implies T_{\text{opt}}=\frac{T}{\sqrt[q+1]{\varepsilon(t_k,T)}}. \tag{26}$$

Usually, a so-called *safety factor* α with $0.5<\alpha<1$ is introduced and a new step-size candidate is calculated by $T_{\text{new}}=\alpha T_{\text{opt}}$ where, in order to avoid too rapid changes, increment and decrement of the step-size are limited according to $\alpha_{\min}\le T_{\text{new}}/T\le\alpha_{\max}$ [19, 20]. Now, if $\varepsilon(t_k,T)\le 1$ holds, the step-size T is *accepted*, time is advanced to $t_{k+1}=t_k+T$ with the according solution $\boldsymbol{w}(t_{k+1})$, and T_{new} is used as a first step-size candidate for T in the next time interval. Otherwise, the step-size T is *rejected*, and the computation starts over again with $\boldsymbol{w}(t_k)$ and the new step-size candidate T_{new}.

Of course, strategies more sophisticated than the one described here do exist in order to control the step-size (see e.g. [21, 22]), each of them having its own pros and cons. However, an investigation or discussion of the different approaches is not within the scope of this paper and we do not follow up this matter any deeper at this point.

The outlined step-size control strategy requires, in addition to the computation of the sought solution $\boldsymbol{w}(t_k+T)$, the determination of a second estimate $\hat{\boldsymbol{w}}(t_k+T)$. For this purpose, a widely used approach is to embed a second RUNGE-KUTTA method in Eqs. (9) by computing

$$\hat{v}(t_{k+1}) = v(t_k) + 2R\hat{\boldsymbol{g}}^{\mathrm{T}}\boldsymbol{i}(t_k), \tag{27}$$

thus specifying a method with unaltered coefficients $\boldsymbol{D}$ and $\boldsymbol{k}$ but with an alternate coefficient vector $\hat{\boldsymbol{g}}$. Here, the estimates $\hat{v}(t_k+T)$ and $v(t_k+T)$ in one time step are always based on the same $v(t_k)$ and the estimate $\hat{v}(t_k+T)$ is disregarded after determination of T_{new}. This kind of approach comes with a comparably low additional implementation effort (e.g. when compared with approaches wich are based on applying one and the same RUNGE-KUTTA method with two different step-sizes) as just one more linear combination of stage currents has to be built and, in particular, Eqs. (9c) have to be evaluated only once.

Although the derivation of the step-size control algorithm was based on the assumption that the embedded

method provides a more accurate estimate than the original one, it is common practice to rather use the above formulas in combination with a lower order method with vector $\hat{\boldsymbol{g}}$ for the determination of a new step-size estimate and a higher order method with vector $\boldsymbol{g}$ for the continuing numerical integration (so-called *local extrapolation* [19]). In the following, we will also make use of this procedure. To this end, a passive diagonally implicit RUNGE-KUTTA method with order q is to be designed with an embedded method of order $q-1$ where the latter, as the estimates it provides are not used for any other computation than a step-size candidate, does not necessarily have to be passive (it might not even be algebraically stable).

6. A passive Runge-Kutta method for automatic step-size control

In the sequel, a suitable passive diagonally implicit RUNGE-KUTTA method for automatic step-size control will be given. Like for most of the commonly used methods, we require the vector $\boldsymbol{k} = [k_1, \ldots, k_s]^{\mathrm{T}}$ to fulfill

$$\boldsymbol{k} = \boldsymbol{D}\boldsymbol{e}. \tag{28}$$

Of course, the order conditions for arbitrary RUNGE-KUTTA methods obeying this condition are known and can be obtained by e. g. applying BUTCHER's formalism [15, 23]. Table 1 displays the resulting conditions for methods up to consistency order four where the product of (column) vectors has to be understood in an element-per-element way. In particular, one must have $\boldsymbol{g}^{\mathrm{T}}\boldsymbol{e} = 1$ for a consistent method (i.e., for a method with an order not less than one), and a comparison of Eqs. (9a) and (9b) shows that Eq. (28) consequently ensures a consistency order one at least for the stage values v_σ.

For passive methods, these order conditions can as well be expressed by employing the parametric representation given in Eqs. (15). By using a suitably adapted version of BUTCHER's formalism, it can be shown that some of the order conditions become redundant in this case such that a reduced set of order conditions can be used here [18]. The relevant conditions for passive methods up to consistency order four are also listed in Table 1.

In addition to the lower number of order conditions, the usage of the parameters introduced in Eqs. (15) simplifies the design of passive methods in another aspect as well. Here, passivity of a method is ensured as long as the parameter r is positive and the parameters $r_1, \ldots, r_s$ are nonnegative. Hence, passivity conditions are completely decoupled while the requirement

$$\boldsymbol{D} + \boldsymbol{D}^{\mathrm{T}} - r\boldsymbol{e}\boldsymbol{e} \geq \boldsymbol{0} \tag{29}$$

– this follows from taking the limit $\psi \to \infty$ within relation (13) in combination with Eq. (10) – induces highly coupled polynomial inequalities in the parameters $d_{\varrho\sigma}$.

A variety of general passive RUNGE-KUTTA methods has already been designed elsewhere [7, 12, 18]. Within this paper, we are mainly interested in finding an appropriate embedded method of maximum order. But, it is known that the consistency order of a passive diagonally implicit RUNGE-KUTTA method cannot exceed four at all, this maximum order four requires at least three stages, and that there exists exactly one fourth-order three-stage method of this kind [7]. The BUTCHER tableau

$$\begin{array}{c|c} \boldsymbol{k} & \boldsymbol{D} \\ \hline & \boldsymbol{g}^{\mathrm{T}} \end{array}$$

of this maximum-order three-stage method is given in Table 2. On the other hand, we will immediately see that there exists no corresponding third-order embedded method. Being of order four, the method of Table 2 fulfills, in particular, the requirements $\boldsymbol{g}^{\mathrm{T}}\boldsymbol{e} = 1$, $\boldsymbol{g}^{\mathrm{T}}\boldsymbol{k} = 1/2$, and $\boldsymbol{g}^{\mathrm{T}}\boldsymbol{k}^2 = 1/3$ from Table 1. For the embedded method, the corresponding requirements would read

$$\hat{\boldsymbol{g}}^{\mathrm{T}} \begin{bmatrix} 1 & k_1 & k_1^2 \\ 1 & k_2 & k_2^2 \\ 1 & k_3 & k_3^2 \end{bmatrix} = \begin{bmatrix} 1 & 1/2 & 1/3 \end{bmatrix}. \tag{30}$$

But, as the method under consideration is not *confluent*, i.e. as it possesses distinct values k_σ, the occcuring VANDERMONDE matrix is regular and the unique solution of these equations is given by $\hat{\boldsymbol{g}} = \boldsymbol{g}$ which clearly is not admissible. Consequently, we need at least four stages in order to obtain a fourth-order method with embedded method of order three.

Table 1. Order conditions for general and passive RUNGE-KUTTA methods up to order four. There holds $\boldsymbol{k} = \boldsymbol{D}\boldsymbol{e}$.

Order	General method	Passive method
$q \geq 1$	$\boldsymbol{g}^{\mathrm{T}}\boldsymbol{e} = 1$	$r\boldsymbol{e}^{\mathrm{T}}\boldsymbol{e} = 1$
$q \geq 2$	$\boldsymbol{g}^{\mathrm{T}}\boldsymbol{k} = 1/2$	$\mathcal{R}\boldsymbol{e} = \boldsymbol{0}$
$q \geq 3$	$\boldsymbol{g}^{\mathrm{T}}\boldsymbol{D}\boldsymbol{k} = 1/6$ $\boldsymbol{g}^{\mathrm{T}}\boldsymbol{k}^2 = 1/3$	$r\boldsymbol{e}^{\mathrm{T}}[\mathcal{S}\boldsymbol{e}]^2 = 1/3$
$q \geq 4$	$\boldsymbol{g}^{\mathrm{T}}\boldsymbol{D}^2\boldsymbol{k} = 1/24$ $\boldsymbol{g}^{\mathrm{T}}\boldsymbol{D}\boldsymbol{k}^2 = 1/12$ $\boldsymbol{g}^{\mathrm{T}}[\boldsymbol{k}[\boldsymbol{D}\boldsymbol{k}]] = 1/8$ $\boldsymbol{g}^{\mathrm{T}}\boldsymbol{k}^3 = 1/4$	$r\boldsymbol{e}^{\mathrm{T}}[\mathcal{S}\boldsymbol{e}]^3 = 0$ $\mathcal{R}\mathcal{S}\boldsymbol{e} = 0$

Table 2. BUTCHER tableau of the fourth-order three-stage passive diagonally implicit RUNGE-KUTTA method.

$\frac{1}{2} + \frac{1}{2\sqrt{2}}$	$\frac{1}{2} + \frac{1}{2\sqrt{2}}$	0	0
$\frac{1}{2}$	$-1 - \sqrt{2}$	$\frac{3}{2} + \sqrt{2}$	0
$\frac{1}{2} - \frac{1}{2\sqrt{2}}$	$1 + \frac{1}{\sqrt{2}}$	$-1 - \sqrt{2}$	$\frac{1}{2} + \frac{1}{2\sqrt{2}}$
	$\frac{1}{3}$	$\frac{1}{3}$	$\frac{1}{3}$

A suitable four-stage method is obtained by starting with a method designed in [12]. Its relevant characteristic parameters for the representation (15) are given by

$$\begin{aligned} r &= \frac{1}{4}, \quad r_1 = \frac{1}{4} + \frac{1}{2\sqrt{3}}, \quad r_2 = r_3 = r_4 = 0, \\ n_{11} &= n_{41} = 1, \quad n_{21} = n_{31} = -1, \\ l_{21} &= l_{31} = l_{42} = r - r_1 = -\frac{1}{2\sqrt{3}}, \\ l_{41} &= l_{32} = r + r_1 = \frac{1}{2} + \frac{1}{2\sqrt{3}}, \end{aligned} \tag{31}$$

The extended BUTCHER tableau for this method, including both $\boldsymbol{g}$ and $\hat{\boldsymbol{g}}$, is depicted in Table 3. Herein, $\hat{\boldsymbol{g}}$ has been constructed as follows. Denote by δ_ν the elements of the vector $\boldsymbol{Dk}$ and supplement Eq. (30) with the condition $\boldsymbol{g}^{\mathrm{T}}\boldsymbol{Dk} = 1/6$ of Table 1 to read

$$\hat{\boldsymbol{g}}^{\mathrm{T}} \begin{bmatrix} 1 & k_1 & k_1^2 & \delta_1 \\ 1 & k_2 & k_2^2 & \delta_2 \\ 1 & k_3 & k_3^2 & \delta_3 \\ 1 & k_4 & k_4^2 & \delta_4 \end{bmatrix} = \begin{bmatrix} 1 & 1/2 & 1/3 & 1/6 \end{bmatrix}. \tag{32}$$

Now, the rank of the matrix in this equation can be computed to be three only, and the equation thus possesses an infinite number of solutions (one of them being $\hat{\boldsymbol{g}} = \boldsymbol{g}$ again). Choosing $\hat{g}_4 = 0$, we obtain the solution given in Table 3.

By construction, the passive method of Table 3 possesses order four while the embedded (non-passive) method possesses order three. Moreover, the passive fourth-order method is singly diagonally implicit – with the aforementioned reduction in computational effort due to equal port resistances in all stages – and its maximum *error constant* – a measure to compare methods possessing the same consistency order – is about 50 times smaller than that of the unique fourth-order three-stage method given in Table 2. Thus, in addition to its applicability in a variable step-size scenario, it may also be viewed as a useful alternative for wave digital simulation with fixed step-size.

Table 3. Extended BUTCHER tableau of a fourth-order passive singly diagonally implicit RUNGE-KUTTA method with embedded third-order (non-passive) method.

$\frac{1}{4}+\frac{1}{4\sqrt{3}}$	$\frac{1}{4}+\frac{1}{4\sqrt{3}}$	0	0	0
$\frac{1}{4}-\frac{1}{4\sqrt{3}}$	$-\frac{1}{2\sqrt{3}}$	$\frac{1}{4}+\frac{1}{4\sqrt{3}}$	0	0
$\frac{3}{4}+\frac{1}{4\sqrt{3}}$	$-\frac{1}{2\sqrt{3}}$	$\frac{1}{2}+\frac{1}{2\sqrt{3}}$	$\frac{1}{4}+\frac{1}{4\sqrt{3}}$	0
$\frac{3}{4}-\frac{1}{4\sqrt{3}}$	$\frac{1}{2}+\frac{1}{2\sqrt{3}}$	$-\frac{1}{2\sqrt{3}}$	$-\frac{1}{2\sqrt{3}}$	$\frac{1}{4}+\frac{1}{4\sqrt{3}}$
	$\frac{1}{4}$	$\frac{1}{4}$	$\frac{1}{4}$	$\frac{1}{4}$
	$\frac{1}{2}$	$\frac{\sqrt{3}-1}{4}$	$\frac{3-\sqrt{3}}{4}$	0

7. Simulation results

In order to test the method derived in the previous section, we have used it to simulate the KIRCHHOFF network of Figs. 1 and 2. This time, the element values were chosen as $R_x = 200\,\Omega$, $C = 47\,\mu\mathrm{F}$, and $L = 10\,\mathrm{mH}$. With this choice, the eigenvalues of the system matrix associated with this network were $\lambda_1 \approx -107\,\mathrm{s}^{-1}$ and $\lambda_2 \approx -19\,900\,\mathrm{s}^{-1}$ and the system equations thus constitute a (mildly) stiff problem. In our simulation, the input signal was a periodic series of $\sin^2$-pulses with amplitude 5 V and a duration of 500 µs (corresponding to a fundamental frequency of 2 kHz) with 20 ms pulse repetition time. The initial values of capacitance voltage and inductance current were chosen in a way that both states were also periodic with period 20 ms. Fig. 6 displays one period of the input signal as well as the exact solutions for capacitance voltage and inductance current within such a time interval.

For the wave digital simulation, the RUNGE-KUTTA method designed in the previous section has been used in connection with the step-size control algorithm outlined in Section 5. Here, the tolerances were $\delta_{\mathrm{abs}} = 1\,\mathrm{nV}$ and $\delta_{\mathrm{rel}} = 10^{-5}$. A safety factor $\alpha = 0.9$ was used while increment and decrement of the step-size were limited ac-

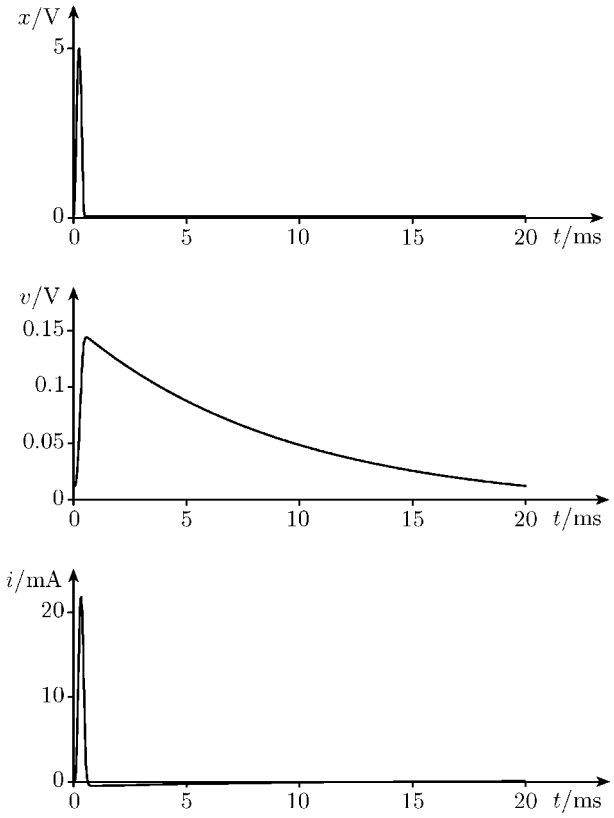

Fig. 6. One period of input signal, voltage across capacitance, and current through inductance for the network shown in Fig. 1.

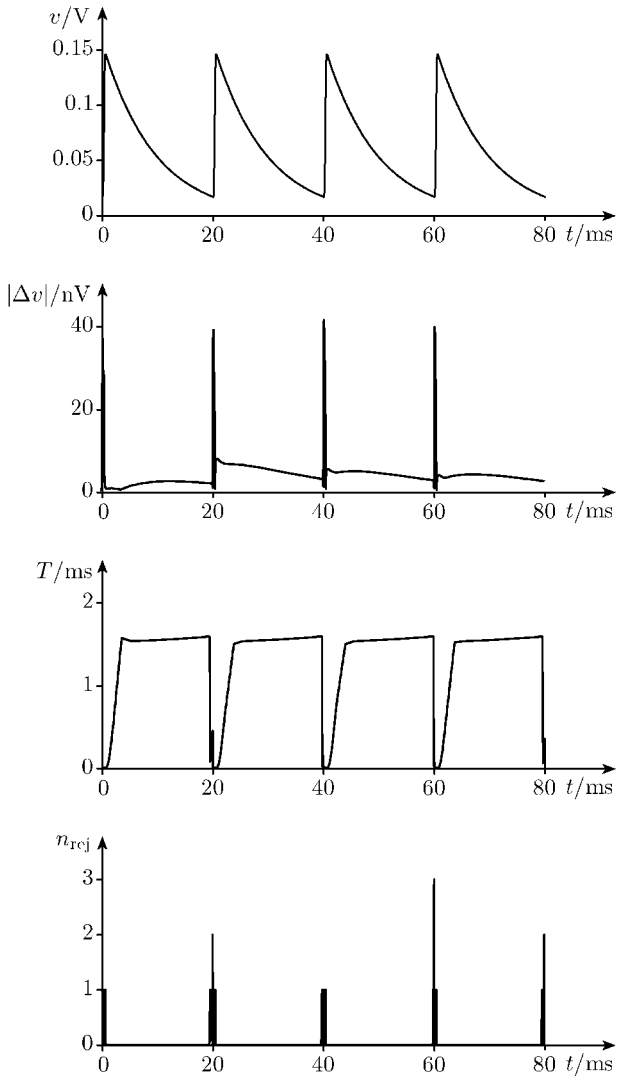

Fig. 7. Simulation results for the circuit in Figs. 1 and 2: voltage v across the capacitance, deviation $|\Delta v|$ from the exact solution given in Fig. 6, step-size T and number n_{rej} of rejected step-sizes.

cording to $0.01 \leq T_{\text{new}}/T \leq 5$. The initial step-size was chosen to be $1/80\,000\,\text{s}$.

In Fig. 7, simulation results for the voltage across the capacitance, its deviation from the exact solution, the automatically adjusted step-size for each time step, and the corresponding number of rejected step-sizes are displayed. As expected, we get small step-sizes for regions where rapid changes in the capacitance voltage (and also in the inductance current not being depicted here) occur while the step-size is kept at a higher level in regions where the transition related to the less negative eigenvalue (i.e. the eigenvalue of smaller magnitude) is dominant.

For reference purposes, we have now performed a wave digital simulation of the circuit using the same RUNGE-KUTTA method with fixed step-size T_1 which has been adjusted in such a manner that the maximum simulation error for both capacitance voltage and inductance

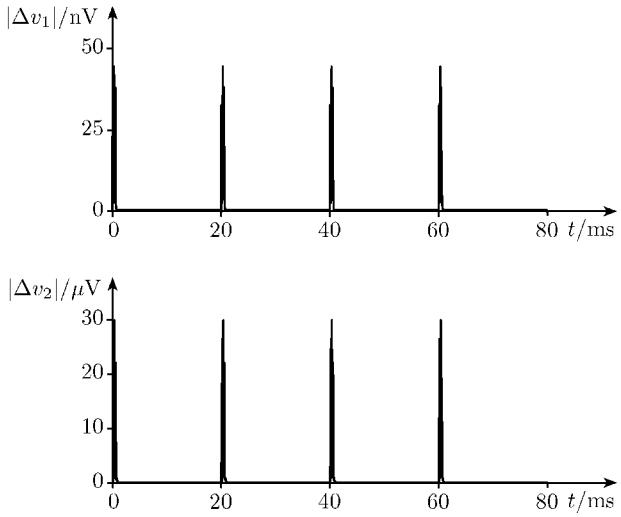

Fig. 8. Simulation errors for the voltage across the capacitance obtained with fixed step-sizes $T_1 = 1/80\,000\,\text{s}$ and $T_2 = 1/13\,000\,\text{s}$.

current take on about the same values as they have done with the variable step-size. Fig. 8 shows the result for the error $|\Delta v_1|$ of the simulated the capacitance voltage which has been obtained by setting $T_1 = 1/80\,000\,\text{s}$. Of course, absolute simulation times vary with software implementation and hardware platform, but in all tested environments, simulation with fixed step-size took approximately six times longer. Hence, we have finally increased the fixed step-size to $T_2 = 1/13\,000\,\text{s}$ which indeed yielded about the same simulation time as we have had with a variable step-size before. As can be seen from $|\Delta v_2|$ shown in Fig. 8, the error now is circa 730 times higher than the one obtained with variable step-size.

8. Conclusions

In this paper, wave digital simulation with controlled variable step-sizes has been discussed. While the problem of applying linear multistep methods, traditionally used for wave digital simulation, with variable step-sizes remains unsolved, the application of suitable RUNGE-KUTTA methods establishes the general possibility of using step-size control within this framework. By a unified treatment of all types of reactive elements, passivity of wave digital simulation can be conserved and thus the advantageous numerical stability properties induced herewith are retained as well.

Step-size control by means of embedded RUNGE-KUTTA methods requires the design of passive methods previously not considered. Parameters of a fourth-order passive singly diagonally implicit four-stage RUNGE-KUTTA method with embedded method of order three have been given. The method has not only been shown to be applicable in a variable step-size scenario, it is also

a useful alternative to previously published methods when it comes to simulating with fixed step-size.

References

[1] Fettweis, A.: Wave digital filters: Theory and practice. Proceedings of the IEEE **74** (February 1986), 270–327.

[2] Fischer, H.D.: Wave digital filters for numerical integration. NTZ Archiv **6** (1984), 37–40.

[3] Meerkötter, K.; Scholz, R.: Digital simulation of nonlinear circuits by wave digital filter principles. Proc. IEEE Intern. Symp. on Circuits and Systems (ISCAS) (1989), 720–723.

[4] Fettweis, A.; Nitsche, G.: Numerical integration of partial differential equations by means of multidimensional wave digital filters. Proc. IEEE Intern. Symp. on Circuits and Systems (ISCAS) **2** (1990), 954–957.

[5] Fettweis, A.: Discrete modelling of lossless fluid dynamic systems. AEÜ Int. J. Electron. Commun. **46** (1992), 209–218.

[6] Meerkötter, K.; Felderhoff, T.: Simulation of nonlinear transmission lines by wave digital filter principles. Proc. IEEE Intern. Symp. on Circuits and Systems (ISCAS) **2** (1992), 875–878.

[7] Ochs, K.: Passive integration methods: Fundamental theory. AEÜ Int. J. Electron. Commun. **55** (2001), 153–163.

[8] Fränken, D.; Ochs, K.: Synthesis and design of passive Runge-Kutta methods. AEÜ Int. J. Electron. Commun. **55** (2001), 417–425.

[9] Ochs, K.: Passive Integrationsmethoden. Aachen: Shaker, 2001. – (Doctoral Dissertation in the Department of Electrical Engineering & Information Technology, University of Paderborn).

[10] Meerkötter, K.; Fränken, D.: Digital realization of connection networks by voltage-wave two-port adaptors. AEÜ Int. J. Electron. Commun. **50** (November 1996), 362–367.

[11] Fränken, D.; Ochs, J.; Ochs, K.: Generation of wave digital structures for connection networks containing ideal transformers. Submitted for publication in: Proc. IEEE Intern. Symp. on Circuits and Systems (ISCAS), 2003.

[12] Fränken, D.: Digitale Simulation physikalischer Systeme mit Methoden der Netzwerktheorie. Düsseldorf: VDI Verlag, 2003. – (Professorial dissertation in the Department of Electrical Engineering & Information Technology, University of Paderborn).

[13] Genin, Y.: A new approach to the synthesis of stiffly stable linear multistep formulas. IEEE Transactions on Circuit Theory **20** (1973), 352–360.

[14] Felderhoff, T.: A new approach to design A-stable linear multistep integration algorithms. Proc. IEEE Intern. Symp. on Circuits and Systems (ISCAS) **5** (1994), 133–136.

[15] Butcher, J.C.: The Numerical Analysis of Ordinary Differential Equations. New York: John Wiley & Sons, 1987.

[16] Dahlquist, G.: A special stability problem for linear multistep methods. BIT **3** (1963), 27–43.

[17] Fränken, D.; Ochs, K.: Numerical stability properties of passive Runge-Kutta methods. Proc. IEEE Intern. Symp. on Circuits and Systems (ISCAS) **3** (2001), 473–476.

[18] Fränken, D.; Ochs, K.: Passive Runge-Kutta methods: Properties, parametric representation, and order conditions. BIT Numerical Mathematics **43** (2003), 339–361.

[19] Hairer, E.; Nørsett, S.P.; Wanner, G.: Solving Ordinary Differential Equations I. New York: Springer, 1993.

[20] Gear, C.W.: Numerical initial value problems in ordinary differential equations. Englewood Cliffs: Prentice-Hall, 1971.

[21] Gustafsson, K.: Control theoretic techniques for stepsize selection in explicit Runge-Kutta methods. ACM Transactions on Mathematical Software **17** (1991), 533–554.

[22] Gustafsson, K.: Control-theoretic techniques for stepsize selection in implicit Runge-Kutta methods. ACM Transactions on Mathematical Software **20** (1994), 496–517.

[23] Butcher, J.C.; Wanner, G.: Runge-Kutta methods: Some historical notes. Applied Numerical Mathematics **22** (1996), 113–151.

Dietrich Fränken was born in Berlin, Germany in 1966. He received the Dipl.-Ing. degree in Electrical Engineering from the Ruhr-University, Bochum, Germany in 1991 and the Dr.-Ing. degree from the University of Paderborn, Germany in 1997, respectively. In 2003, he obtained his postdoctoral lecture qualification, again from the University of Paderborn, Germany. Currently, he is a design engineer in the Competence Center Sensor Software of EADS Deutschland GmbH, Ulm, Germany. Research interests include system theory, estimation, and digital signal processing.

Karlheinz Ochs was born in Lingen, Germany in 1968. He received the Dipl.-Ing. degree and the Dr.-Ing. degree in Electrical Engineering both from the University of Paderborn, Germany, in 1996 and 2001, respectively. From 2001 to 2002, he was a design engineer at the Technology and Development Center, Siemens AG, Bruchsal, Germany. Currently, he is a postdoctoral researcher at the Department of Electrical Engineering and Information Technology/Communications Engineering at the Ruhr-University, Bochum, Germany. Research interests include system theory and digital signal processing.